J. Phys. Chem. A **2009,** *113,* 5406–5413

Ab Initio Study of Structural, Electronic, and Magnetic Properties of $V_n(C_{60})_m$ Complexes

Xiuyun Zhang,[†] Jinlan Wang,*,[†] and Xiao Cheng Zeng[‡]

Department of Physics, Southeast University, Nanjing 211189, P. R. China, and Department of Chemistry and Nebraska Center for Materials and Nanoscience, University of Nebraska, Lincoln, Nebraska 68588

Received: July 21, 2008; Revised Manuscript Received: February 5, 2009

We have studied structural, electronic, and magnetic properties of transition-metal−fullerene complexes $V_n(C_{60})_m$, $(n, m) = (1, 1), (1, 2), (2, 3), (3, 4), (4, 4)$, by means of a density functional theory method. We have examined relative stabilities of complexes with different V−C_{60} binding sites (V atoms are bound to either pentagonal or hexagonal rings of C_{60}) and with different stacking configurations (linear or nonlinear). The linearly stacked sandwichlike complexes with V atoms binding to hexagonal rings of C_{60} are the most stable for $(n, m) = (n, n + 1)$, although nonlinearly stacked configurations can be energetically competitive. For $(n, m) = (1, 1)$, the V atom tends to bind to a pentagonal ring of the C_{60} molecule. For $(n, m) = (4, 4)$, a riceball-like structure is found to be the most stable. Except for $(n, m) = (1, 1)$, the lowest-energy structures of the complexes are generally in their lowest spin states.

I. Introduction

Low-dimensional compounds that are comprised of transition-metal (TM) atoms and organic molecules such as cyclopentadienyl (C_5H_5) and benzene ($Bz = C_6H_6$) have been extensively studied for many years both experimentally and theoretically.[1−29] An example of such compounds is the TM−Bz complex, whose structure can be either multidecker sandwichlike for early TMs such as Sc, Ti, and V or riceball-like for late TMs such as Fe, Co, and Ni.[2−12] Novel magnetic properties in V_nBz_{n+1} have been observed in Stern−Gerlach molecular beam deflection experiments and predicted from density functional theory (DFT) calculations.[4,18−20] TM−C_5H_5 multidecker sandwichlike complexes have also been synthesized despite the fact that pure C_5H_5 radicals are difficult to produce in the gas phase.[27−29] Buckminsterfullerene C_{60} is a versatile ligand for interacting with TM atoms to make metal−ligand compounds because it has 20 six-membered rings and 12 five-membered rings. Nakajima and coworkers[3,30,31] have synthesized $TM_n(C_{60})_m$ cations using the laser vaporization method. They predicted that the $TM_n(C_{60})_m^+$ (TM = V, Ti, and Sc) cationic complexes exhibit sandwichlike structures for $m = n + 1$, $n = 1$ to 3 or ringlike structures for $m = n$, $n = 4$ to 5. The chemical probe experiment further suggested that the TM atoms may bind to hexagonal rings of C_{60} molecules in these complexes. Theoretically, Andriotis et al.[32,33] have investigated small $TM_n(C_{60})_m$ (TM = V, Ni, $n + m \leq 4$) clusters with molecular dynamics and ab initio methods and found that C_{60} acts as η^3 or η^2 ligands toward Ni but as η^6 ligands toward the V atom in the $TM(C_{60})_2$ clusters. However, it is still challenging to infer geometric structures of the $TM_n(C_{60})_m$ complexes directly. Therefore, complementary ab initio theoretical studies are needed to explore geometric, electronic, and magnetic properties of the $TM_n(C_{60})_m$ complexes.

In this article, we have systematically investigated structural, electronic, and magnetic properties of $V_n(C_{60})_m$ complexes for $(m, n) = (1, 1), (1, 2), (2, 3), (3, 4)$, and $(4, 4)$, which have been synthesized experimentally.[3,30,31] We studied various geometries of these complexes to search for the lowest-energy structures; geometries include V atoms binding to pentagonal or hexagonal carbon rings (denoted as η^5-ligand or η^6-ligand structure, respectively) and linear or nonlinear multidecker (ringlike) configurations of C_{60} molecules. Among these geometries, the η^6-ligand structures are the most stable, although linear and nonlinear structures are also energetically competitive for $(m, n) = (n, n + 1)$. For $(m, n) = (1, 1)$, the η^5-ligand structure is the most stable. For $(m, n) = (4, 4)$, a riceball-like structure is much more stable than the ringlike structure.

II. Computational Methods

For ab initio calculations, we used a DFT method with the Becke and Lee−Yang−Parr exchange-correlation functional (BLYP),[34,35] a double numerical basis set including d polarization functions (DNDs), and a relativistic semicore pseudopotential (DSPP), all implemented in the DMol package.[36] Geometry optimizations were carried out using the Broyden−Fletcher−Goldfarb−Shanno algorithm with a fine accuracy, that is, the convergence criterion of 10^{-3} a.u. on the gradient and displacement and 10^{-6} a.u. for the total energy and electron density.

To identify the lowest-energy structure, various geometric configurations, either linearly or nonlinearly stacked, with different binding sites between V atoms and C_{60} molecules were considered. To obtain the ground spin states, the magnetic moment was first allowed to optimize freely to the energetically favored spin state (S_z); then, the neighboring spin states ($S_z \pm 2$) were fixed during the optimization to confirm that the obtained spin state is the most energetically preferred. All structures were fully optimized without using symmetry restriction.

The selection of the BLYP/DND/DSPP method was justified on the basis of simple benchmark systems, namely, a single V atom, a V_2 dimer, a C_{60} molecule, and two small V−Bz compounds (VBz, VBz_2). As a comparison, another two GGA functionals of PW91 and PBE with the same basis sets were also considered. The theoretical and experimental results are presented in Table 1. As displayed in Table 1, the BLYP/DND/DSPP gave the best agreement to the experimental data for the

---

* Corresponding author. E-mail: jlwang@seu.edu.cn.

[†] Southeast University.

[‡] University of Nebraska.

10.1021/jp8064272 CCC: $40.75

TABLE 1: Comparison of (BLYP/PBE/PW91)/DNP with Experimental (EXP) Studies[a]

	properties	BLYP	PBE	PW91	EXP
V	IP (eV)	6.851	6.555	6.649	6.746[37]
V_2	R_{V-V} (Å)	1.80	1.78	1.78	1.77[38]
	IP (eV)	6.33	6.34	6.37	6.35[37]
C_{60}	BE (eV)	7.06	7.54	7.55	7.04[39]
	R_{C-C} (Å)	1.459/1.404	1.439/1.387	1.439/1.386	1.458/1.401[40]
VBz	IP (eV)	5.604	5.827	5.861	5.14[2]
	BE (eV)	0.714	1.721	1.757	0.79[14]
VBz_2	IP (eV)	5.730	5.802	5.930	5.75(3)[2]
	BE_{VBz} (eV)	2.812	3.428	3.453	3.19[14]

[a] R_{C-C} and R_{V-V} are the equilibrium interatomic distances, IP is the ionization potential, and BE is the binding energy of C_{60}, BE = $[60E(C) - E(C_{60})]/60$; of VBz, BE = $E(V) + E(Bz) - E(VBz)$; and of VBz_2, $BE_{VBz} = E(Bz) + E(VBz) - E(VBz_2)$.

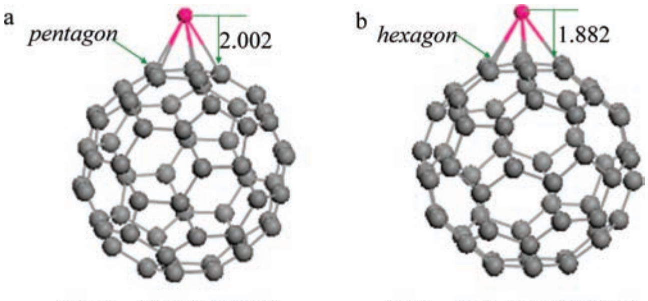

(a) C_{5v}, M=6, ΔE=0 eV (b) C_s, M=4, ΔE=0.078 eV

Figure 1. Optimized structures of VC_{60}, the distance (Å) between the V atom and the C_{60} molecule, R_{V-L}, group symmetry, spin multiplicity (M), and relative energy with respect to the lowest-energy structure, ΔE.

tested systems and therefore was chosen to investigate properties of the V−C_{60} complexes.

III. Results and Discussion

The optimized structures of $V_n(C_{60})_m$, n, m = 1 to 4, obtained at BLYP/DND level are displayed in Figures 1−5, and the structure/symmetry, spin-multiplicity, bond length, relative energy, and HOMO−LUMO gap of low-lying isomers of the complexes are presented in Tables 2−4 and Table S1 in the Supporting Information.

A. Geometry. ***VC_{60}* Complex.** Two initial configurations were constructed for this complex: (a) a C_{3v} configuration with the V atom binding to a hexagonal ring of C_{60} (η^6-ligand) and (b) a C_{5v} configuration (η^5-ligand) where the V atom is located on the C_5 axis of C_{60}. The lowest-energy configuration is the one with the η^5-ligand, and it is in the sextet state with C_{5v} symmetry (Figure 1a). The V atom is about 2.002 Å from the mass center of the five-membered ring (R_{V-L5}). Because of the V−C_{60} interaction, the five-membered carbon ring binding to V is expanded and exhibits the largest C−C bond lengths (R_{C-C}) of 1.462 Å. Other C−C bond lengths in C_{60} vary from 1.451 to 1.459 Å for the 5/6 edges and from 1.401 to 1.416 Å for the 6/6 edges. The η^6-ligand configuration is in the quartet state with C_s symmetry (Figure 1b), and this configuration is 0.078 eV higher in energy than the η^5-ligand configuration. The distance between V and the mass center of the six-membered ring (R_{V-L6}) is 1.882 Å, 0.12 Å shorter than the corresponding distance in the η^5-ligand structure. The R_{C-C} distances are about 1.400 to 1.479 Å in the six-membered ring that binds to V and 1.399 to 1.471 Å in other rings. The chemical probe experiment suggested that the V atom tends to bind to the hexagonal ring of C_{60} in the VC_{60}^+ cation.[3,30,31] The inconsistency between theory and experiment might be due to the two nearly degenerate VC_{60} structures (ΔE = 0.078 eV); both structures thereby may be involved in the reaction experiment.

***$V(C_{60})_2$* Complex.** Five initial configurations (Figure 2) were constructed for the smallest sandwichlike complex: (a) a normal η^6-ligand structure with D_{3d} symmetry, where the V atom binds two opposing six-membered rings; (b) a staggered sandwichlike structure with D_3 symmetry, in which one C_{60} molecule is rotated by 30° along the C_3 axis with respect to the other C_{60}; (c) a normal D_{5h} η^5-ligand structure with the V atom binding to two opposing five-membered rings; (d) a staggered sandwichlike structure in D_{5d} symmetry with one C_{60} molecule rotated by 36° about the C_5 axis with respect to the other one; (e) a mixed-ligand sandwichlike structure ($\eta^5-\eta^6$-ligand) where the V atom is binding to one five-membered ring of one C_{60} and one six-membered ring of another C_{60}.

The most stable structure of $V(C_{60})_2$ is the normal η^6-ligand sandwichlike structure with C_2 symmetry in the doublet state (Figure 2a), which is slightly distorted from the D_{3d} structure by rotating one C_{60} molecule along the C_3 axis by about 8°. The R_{V-L6} is 1.855 Å, and R_{C-C} is 1.422 Å for the 6/6 edges and 1.452 Å for the 5/6 edges in the six-membered rings binding to V. Other R_{C-C} distances are about 1.399 to 1.422 Å for the 6/6 edges and 1.451 to 1.466 Å for the 5/6 edges. The staggered η^6-ligand sandwichlike structure is also in the doublet state with D_3 symmetry (Figure 2b), and it is only 0.092 eV higher in energy than the normal (C_2) one with very close R_{V-L6} and R_{C-C} values, as shown in Table 2. The normal η^5-ligand structure (D_{5h}) (Figure 2c) is in the sextet state and is 0.156 eV higher in energy than the lowest-energy η^6-ligand sandwichlike structure. The R_{V-L5} is lengthened to 2.056 Å, and the R_{C-C} distances are about 1.461 Å in the rings binding to V, and are about 1.400 to 1.461 Å in other rings of C_{60}. The staggered η^5-ligand structure with D_{5d} symmetry (Figure 2d) is 0.002 eV higher in energy than the D_{5h} structure with nearly the same R_{V-L5} and R_{C-C}.

The mixed-ligand structure is in the quartet state with C_s symmetry (Figure 2e), and the R_{V-L6} and R_{V-L5} are 1.895 and 2.028 Å, respectively. However, the mixed-ligand structure has much higher energy (ΔE = 0.323 eV) than that of the lowest-energy η^6-ligand structure.

***$V_2(C_{60})_3$* Complex.** Seven different initial configurations were constructed for this complex: (a) a normal η^6-ligand sandwichlike structure with D_{3d} symmetry; (b) a staggered η^6-ligand S_6 structure with the middle C_{60} rotated by 30° with respect to the two C_{60} at the ends; (c) a normal η^5-ligand sandwichlike structure with C_{5v} symmetry; (d) a staggered η^5-ligand structure with D_{5d} symmetry and one terminal C_{60} rotated by 36° with respect to the other one; (e) a mixed $\eta^5-\eta^6$-ligand structure with the V atoms sandwiched between the six- and five-membered rings of two neighbor C_{60}; (f,g) two nonlinearly stacked structures with the V atoms located between two six-membered rings of neighbor C_{60}.

TABLE 2: Point Group Symmetry (PGS), Spin Multiplicities (*M*), Relative Energies with Respect to the Lowest-Energy Structures (Δ*E*), HOMO−LUMO Gap (Δ), C−C Bond Lengths (R_{C-C}), V−C_{60} Distance (R_{V-L}) Defined as the Distance from the V Atom to the Mass Center of the Five-Membered or Six-Membered Carbon Ring Binding to V, Binding Energy (BE) per V Atom, and Computed Vertical (VIP) and Measured (IP_{exptl}) Ionization Potential of VC_{60} and $V(C_{60})_2$

system	PGS	*M*	Δ*E* (eV)	Δ (eV)	R_{C-C} (Å)	R_{V-L} (Å)	BE (eV)	VIP (eV)	IP_{exptl} (eV)[30]
VC_{60}	C_{5v}−a	6	0	0.155	1.401−1.462	2.002	0.822	5.920	5.92−6.42
	C_s−b	4	0.078	0.375	1.399−1.479	1.882	0.744	6.400	
$V(C_{60})_2$	C_2−a	2	0	0.585	1.399−1.466	1.855	2.534	6.099	5.82 ± 0.005
	D_3−b	2	0.092	0.561	1.399−1.467	1.860	2.443	6.081	
	D_{5h}−c	6	0.156	0.242	1.400−1.461	2.056	2.379	5.895	
	D_{5d}−d	6	0.158	0.241	1.400−1.460	2.055	2.377	5.896	
	C_s−e	4	0.323	0.128	1.399−1.474	2.028, 1.895	2.212	5.964	

TABLE 3: Data of $V_2(C_{60})_3$ Complex as in Table 2

PGS	*M*	Δ*E* (eV)	Δ (eV)	R_{C-C} (Å)	R_{V-L} (Å)	BE (eV)	VIP (eV)	IP_{exptl}[30]
D_{3d}−a	1	0	0.529	1.400−1.468	1.856, 1.862	2.494	5.738	5.92−6.42
	3	0.011	0.390	1.399−1.467	1.855, 1.862	2.489	5.733	
S_6−b	1	0.063	0.503	1.399−1.468	1.856, 1.863	2.463	5.726	
	3	0.075	0.372	1.399−1.468	1.856, 1.862	2.457	5.714	
C_{5v}−c	11	0.185	0.041	1.400−1.460	2.054, 2.055, 2.058	2.402	5.577	
D_{5d}−d	11	0.187	0.041	1.400−1.461	2.056, 2.058	2.401	5.577	
C_s−e	7	0.362	0.205	1.398−1.474	1.887−2.021	2.314	5.768	
C_1−f	3	0.013	0.419	1.398−1.466	1.856−1.862	2.488	5.760	
	1	0.020	0.539	1.399−1.466	1.855, 1.859, 1.862	2.485	5.770	
C_1−g	1	0.053	0.519	1.399−1.467	1.855−1.860	2.468	5.808	
	3	0.057	0.427	1.398−1.467	1.855, 1.858, 1.859	2.466	5.805	

TABLE 4: Data of $V_3(C_{60})_4$ and $V_4(C_{60})_4$ Complexes as Shown in Table 2

system	PGS	*M*	Δ*E* (eV)	Δ (eV)	R_{C-C} (Å)	R_{V-L} (Å)	BE (eV)	VIP (eV)	IP_{exptl}[30]
$V_3(C_{60})_4$	D_{3d}−a	2	0	0.380	1.398−1.468	1.852, 1.861, 1.865	2.490	5.534	5.92−6.42
		4	0.014	0.312	1.398−1.467	1.852, 1.861, 1.865	2.485	5.585	
	C_1−b	2	0.108	0.376	1.399−1.468	1.837−1.863	2.454	5.546	
		4	0.125	0.314	1.398−1.468	1.837−1.862	2.448	5.549	
	C_1−c	2	0.114	0.415	1.399−1.467	1.844−1.864	2.452	5.645	
		4	0.131	0.337	1.398−1.467	1.842−1.864	2.446	5.640	
	C_1−d	2	0.024	0.396	1.398−1.466	1.851−1.863	2.482	5.565	
		4	0.028	0.327	1.398−1.466	1.851−1.863	2.481	5.638	
	C_1−e	2	0.037	0.398	1.399−1.466	1.845−1.869	2.478	5.660	
		4	0.042	0.326	1.399−1.467	1.846−1.866	2.476	5.582	
$V_4(C_{60})_4$	a	1	0	0.129	1.396−1.499		3.412	5.812	
	b	1	3.708	0.328	1.398−1.467	1.856−1.864	2.486	5.623	

The most stable structure of $V_2(C_{60})_3$ is the normal η^6-ligand sandwichlike structure with D_{3d} symmetry and is in the singlet state (Figure 3a). Its triplet state is only 0.011 eV higher in energy. The R_{C-C} distances are 1.422 Å for the 6/6 edges and 1.453 Å for the 5/6 edges in the carbon rings binding to V and are about 1.400 to 1.468 Å for the rest. The V atoms are 1.856 and 1.862 Å to the hexagonal rings of the end and middle C_{60}. The optimized staggered η^6-ligand sandwichlike structure (Figure 3b) retains the S_6 symmetry in the singlet state. Similar to $V(C_{60})_2$, this staggered structure is close in energy to the normal one (0.063 eV difference). The lowest-energy η^5-ligand sandwichlike structure has C_{5v} symmetry (Figure 3c), and it is about 0.185 eV higher in energy than the lowest-energy η^6-ligand structure. Remarkably, the most favored spin state has a magnetic moment of 10 μ_B. The staggered structure (Figure 3d, in D_{5d}) has the same magnetic moment of 10 μ_B, and it is only 0.002 eV higher than its normal sandwichlike structure. The mixed-ligand structure (Figure 3e) also has a high magnetic moment of 6 μ_B, but it has much higher energy ($\Delta E = 0.362$ eV) compared with the lowest-energy η^6-ligand structure.

The two nonlinear η^6-ligand sandwichlike structures (Figure 3f,g) are in the triplet and singlet states, respectively, and they are about 0.013 and 0.053 eV higher in energy than the lowest-energy η^6-ligand structure. The singlet state of structure f is

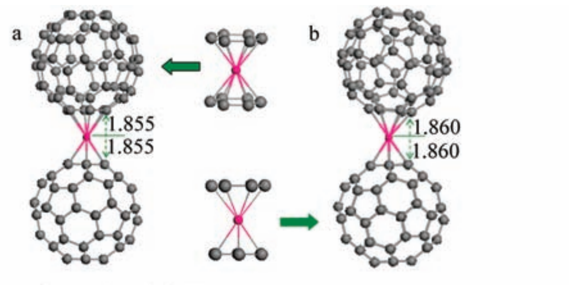

C_2, *M*=2, Δ*E*=0 eV D_3, *M*=2, Δ*E*=0.092eV

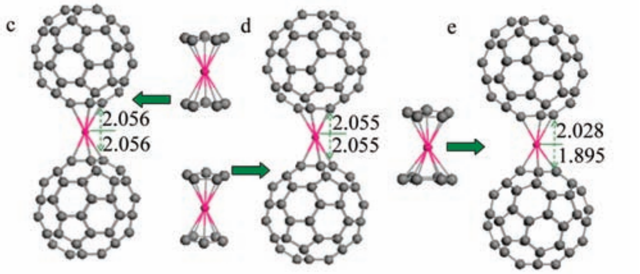

D_{5h}, *M*=6, Δ*E*=0.156 eV D_{5d}, *M*=6, Δ*E*=0.158eV C_s, *M*=4, Δ*E*=0.323 eV

Figure 2. Optimized structures of $V(C_{60})_2$.

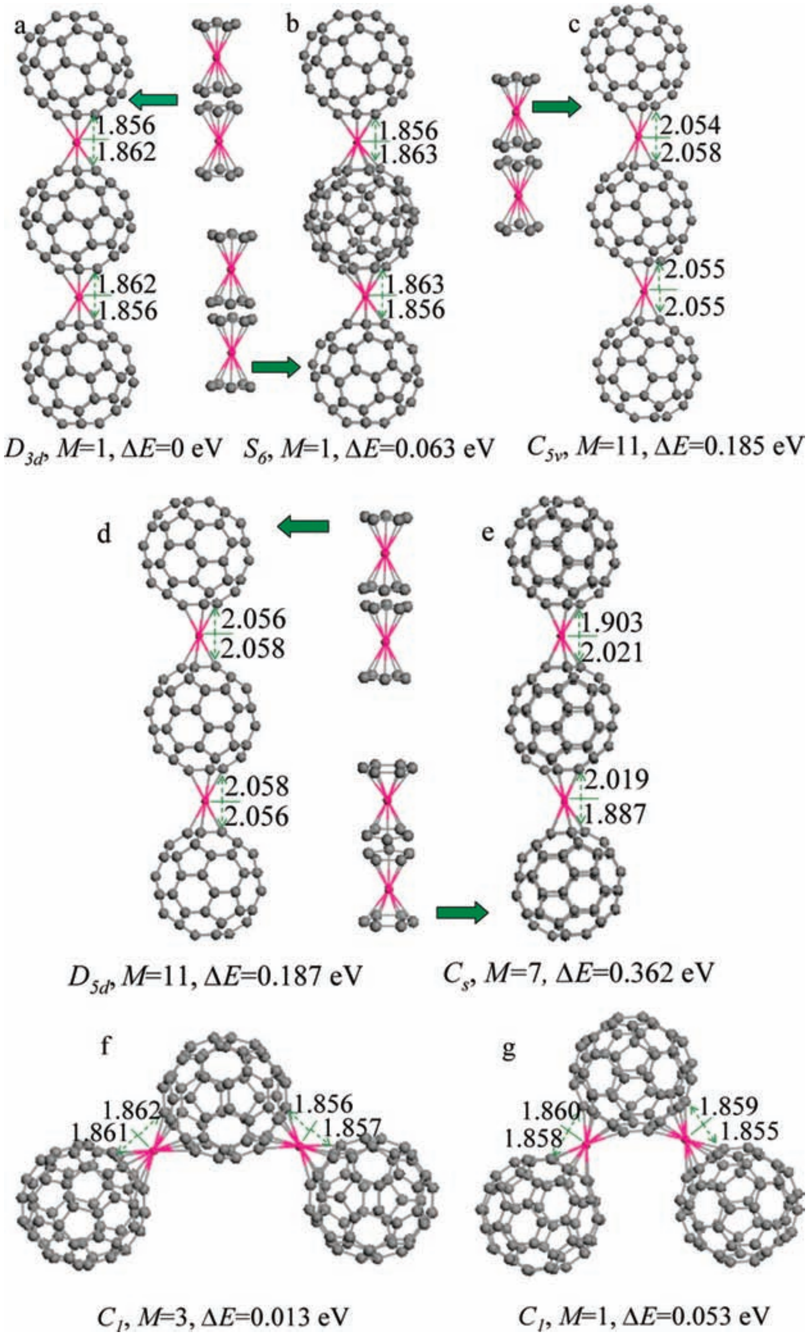

D_{3d}, M=1, ΔE=0 eV S_6, M=1, ΔE=0.063 eV C_{5v}, M=11, ΔE=0.185 eV

D_{5d}, M=11, ΔE=0.187 eV C_s, M=7, ΔE=0.362 eV

C_1, M=3, ΔE=0.013 eV C_1, M=1, ΔE=0.053 eV

Figure 3. Optimized structures of $V_2(C_{60})_3$.

degenerate with the triplet state with an energy difference of only 0.007 eV. The triplet state of structure g is only 0.004 eV higher in energy than the singlet state. Therefore, for nonlinear structures f and g, the most stable state can be in either the singlet or triplet state because of such small energy differences.

As shown above, there are some common structural characteristics in $V(C_{60})_2$ and $V_2(C_{60})_3$: (1) the V atom tends to bind to the six-membered ring of C_{60}; (2) the binding of V atoms to one or two five-membered rings is less stable, but it can induce a higher spin moment; (3) the rotation of one C_{60} molecule does not significantly affect the overall stability of the complex, although high energy barriers may exist between different rotational states.

$V_3(C_{60})_4$ Complex. Because the structures with V atoms binding to five-membered rings or to one C_{60} rotated with respect to other C_{60} are energetically unfavorable, we considered only normal sandwichlike structures with the V atoms binding to hexagonal rings of C_{60}. Besides the linear structure, four nonlinear structures with the V atoms binding to six-membered rings of C_{60} were considered. All five optimized structures are displayed in Figure 4.

The most stable structure is a linear sandwichlike structure with D_{3d} symmetry in the doublet state (Figure 4a); the quartet state is less stable by 0.014 eV in energy. In the doublet state, the R_{V-L6} distances are 1.852, 1.861, and 1.865 Å; the R_{C-C} distances are 1.452 and 1.453 Å for the 5/6 edges and 1.422 and 1.423 Å for the 6/6 edges in the rings binding to V. Other R_{C-C} distances are about 1.398 to 1.468 Å.

When a $V-C_{60}$ unit is located off the main axis (Figure 4b,c), the most favorable spin states are still doublets, but the energies of these two configurations are 0.108 and 0.114 eV higher, respectively, compared with that of the most stable structure (Figure 4a). The structure (Figure 4d) with two parallel $V(C_{60})_2$ units connected by a V atom is also in the doublet state, and it

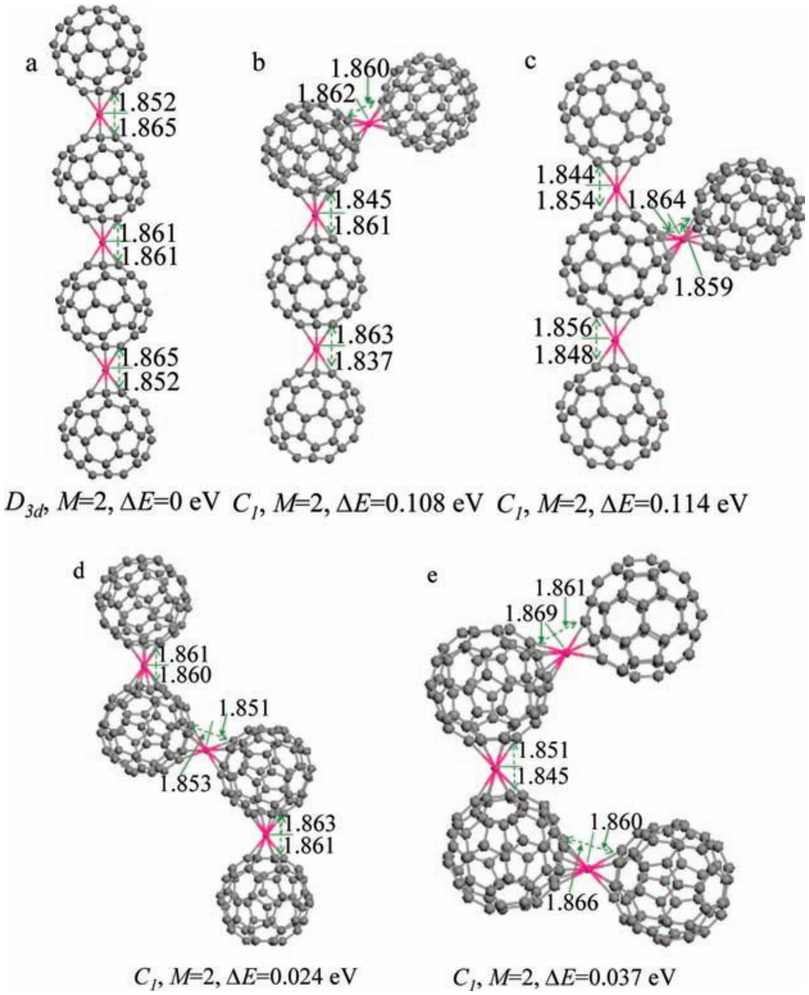

D_{3d}, M=2, ΔE=0 eV C_1, M=2, ΔE=0.108 eV C_1, M=2, ΔE=0.114 eV

C_1, M=2, ΔE=0.024 eV C_1, M=2, ΔE=0.037 eV

Figure 4. Optimized structures of $V_3(C_{60})_4$.

is 0.024 eV higher in energy than the lowest-energy structure. An open-ring structure (Figure 4e) is in the doublet state and is 0.037 eV higher in energy than the lowest-energy structure. As in the case of $V_2(C_{60})_3$, the quartet states for all five structures of $V_3(C_{60})_4$ are close in energy to the doublets (only 0.004 to 0.017 eV in energy differences). The lower stabilities of structures declined from D_{3d} might be attributed to the least strain−strain interaction in the linear sandwich D_{3d} structure. Among the four nonlinear structures (Figure 4b−e), because the $V(C_{60})_2$ subunits are more symmetrically bonded to each other in the structure shown in Figure 4d,e, they are expected to have less strain energy and thus are more stable than the two structures shown in Figure 4b,c.

***$V_4(C_{60})_4$* Complex.** Chemical probe experiments suggested that no V atom is located in the outer region of $V_4(C_{60})_4^+$.[3,30,31] As such, we constructed two initial configurations: (a) a ringlike structure with the V atoms located between C_{60} molecules, and (b) a riceball-like structure with four V atoms forming a tetrahedron unit, which is surrounded by four C_{60} molecules. The riceball-like structure in the singlet state is more stable among the two structures at various spin states, as in the case of the Co_4Bz_4 cluster.[21] The ringlike structure favors the singlet state but it has much higher energy (3.708 eV) than the riceball-like structure. These results are in disagreement with experimental suggestion that a ringlike structure is more likely for the cationic complex.[3,30,31] As displayed in Figure 5a, the riceball-like structure is actually distorted with each V atom binding to either a C−C bond or one C atom. The V−V and V−C bond lengths are about 2.252 to 2.469 and 2.131 to 2.689 Å, respectively. The V−V bond lengths here are a bit larger than those of the bare V tetrahedron[37] (2.206 Å). The ringlike structure has bond lengths similar to those of the sandwichlike clusters (Figure 5b), in which R_{V-L} distances are 1.856 to 1.864 Å and R_{C-C} distances are 1.398 to 1.467 Å, with those in the 5/6 edges longer than those in the 6/6 edges.

B. Size-Dependent Energetic, Electronic, and Magnetic Properties. The average binding energy (BE(n, m)) per V atom for a $V_n(C_{60})_m$ complex with respect to individual V atom and C_{60} molecule is computed using the formula $BE(n, m) = \{nE[V] + mE[C_{60}] - E[V_n(C_{60})_m]\}/n$, where the $E[\cdot]$ is the total energy of a relaxed $V_n(C_{60})_m$, a single C_{60} molecule, or a V atom. The BE per V atom of the most stable structures quickly increases from 0.822 eV for VC_{60} to 2.534 eV for $V(C_{60})_2$, but then decreases a little to 2.494 eV for (2, 3) and to 2.490 eV for (3, 4). For (4, 4), the BE per V atom is 3.412 eV, which is significantly higher than that of other sandwichlike clusters. However, the BE per V atom of the ringlike structure is only 2.486 eV, close to those of sandwichlike clusters. This result can be understood from their different structural characteristics. In sandwichlike or ringlike structures, the V atoms are located between C_{60} molecules, and their binding interaction is relatively weak. When the V atoms form a metal cluster and are surrounded by C_{60} molecules in the riceball-like structure, the orbital overlapping between V and V as well as V and C_{60} is much larger, giving rise to much higher BE.

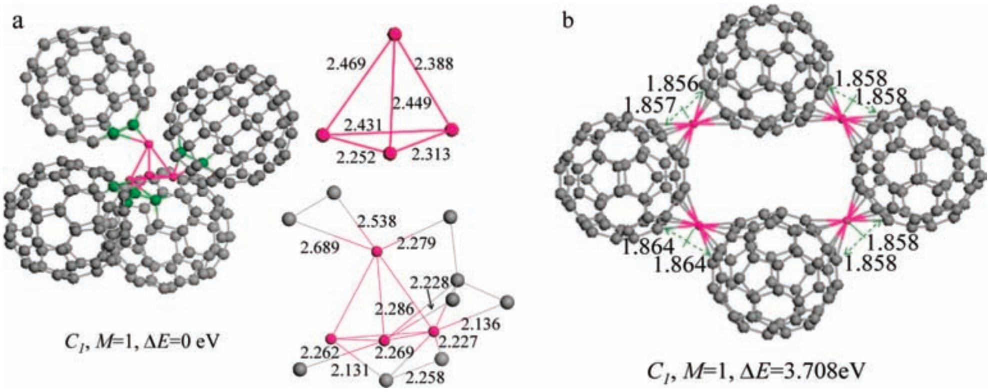

Figure 5. Optimized structures of the $V_4(C_{60})_4$ cluster, as in Figure 1.

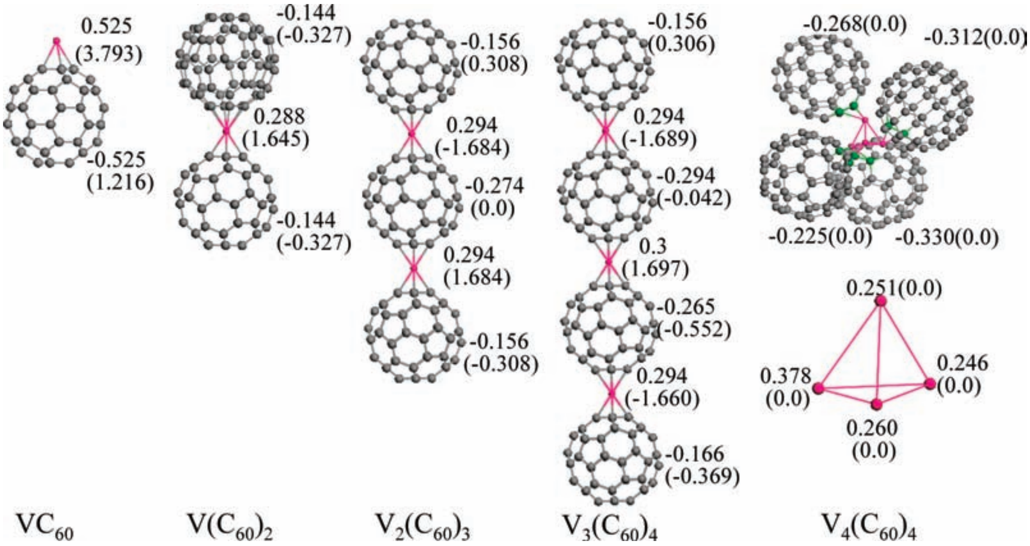

Figure 6. Mulliken charge (spin) on V atoms and C_{60} molecules of the lowest-energy structures of $V_n(C_{60})_m$. The number in parentheses is the local magnetic moment in μ_B.

The HOMO−LUMO gaps of the complexes studied are all relatively small (Tables 2−4), indicating that these complexes may be highly reactive. The maximum HOMO−LUMO gap among the most stable structures is 0.585 eV for $V(C_{60})_2$, suggesting that $V(C_{60})_2$ is relatively more stable than other complexes.

The vertical ionization potentials (VIPs) of low-lying complexes are also computed and presented in Tables 2−4. The VIP of the lowest-energy structures shows a peak value (6.099 eV) at $V(C_{60})_2$ and a minimum at $V_3(C_{60})_4$. The measured IPs are well reproduced for (1, 1) but have some discrepancies with the calculated VIPs for (1, 2), (2, 3), and (3, 4).[30] As shown above, several low-lying isomers for each complex were identified. (See Tables 2−4.) For example, the η^6-ligand structure of VC_{60} is only 0.078 eV higher in energy than the η^5-ligand structure. Similarly, energy differences between nonlinear and linear structures are small, less than 0.06 eV for (2, 3) and 0.12 eV for (3, 4). These nearly isoenergy structures may coexist and contribute to the measured photoionization spectra. One can see from Tables 2−4 that the computed VIPs of some low-lying isomers are quite close in value to the measured ones.

Except for the (1, 1) complex, which is in the sextet state, other complexes favor the lowest spin states, that is, either the singlet states for complexes with an even number of electrons or the doublet states for complexes with an odd number of electrons. We have shown that for the (1, 1) complex, the V atom actually binds to a five-membered ring, whereas for the complexes (n, n + 1), the V atoms bind to six-membered rings. We have also shown that the η^5-ligand configurations favor higher magnetic moments. For example, the η^5-ligand and the mixed $\eta^5-\eta^6$-ligand structures of $V_2(C_{60})_3$ possess magnetic moments of 10 and 6 μ_B, respectively. Therefore the (1, 1) complex is also expected to exhibit a high magnetic moment. The Mulliken spin distributions on localized V atoms and C_{60} molecules are shown in Figure 6. In VC_{60}, the V atom ferromagnetically couples to C_{60} with the local moments being 3.793 and 1.216 μ_B, respectively. In the case of $V(C_{60})_2$, the magnetic moment of the V atom is reduced to 1.645 μ_B, which is antiparallel with the two C_{60} with small negative values (−0.327 μ_B). Therefore, the total moment of the cluster is only 1 μ_B. As for $V_2(C_{60})_3$ and $V_3(C_{60})_4$, the local moments on V atoms and C_{60} molecules are similar to those in $V(C_{60})_2$, whereas the magnetic coupling between V atoms and between V atoms and C_{60} molecules is antiparallel. Therefore, the magnetic moments of these clusters are very small. In $V_4(C_{60})_4$, the local moments of every part are zero.

The Mulliken charge distribution on each V atom and C_{60} molecule of the lowest-energy structures of $V_n(C_{60})_m$ can be used to characterize the interaction between V and C_{60} (Figure 6). All V atoms have positive charge, and C_{60} ligands possess negative charge. The charge on the inner C_{60} molecules is almost twice that at the end in the sandwichlike complexes. This is because inner C_{60} molecules are located between two V atoms,

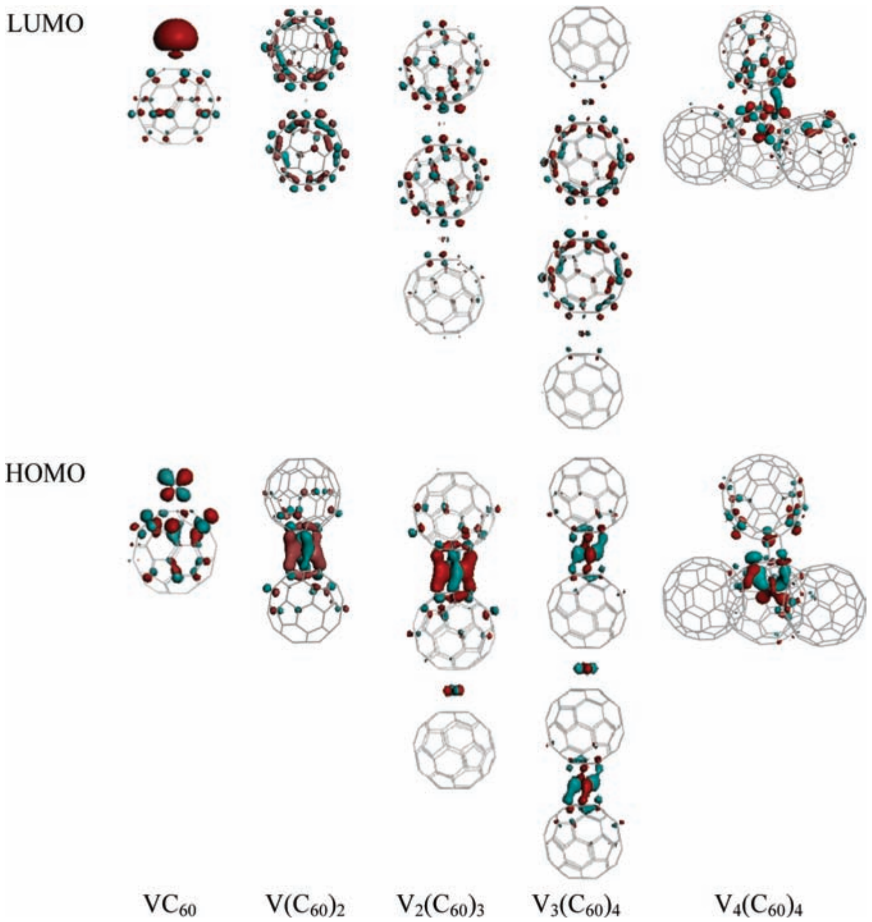

Figure 7. Isodensity surface of HOMOs (bottom) and LUMOs (top) of the lowest-energy structures of $V_n(C_{60})_m$.

and the charge transfer should be more pronounced. In (4, 4), the four V atoms and C_{60} molecules have similar charges due to its riceball-like structure (with tetrahedral unit of V surrounded by C_{60}). The charge distributes nearly symmetrically about the principal axis of the complexes, giving a small dipole moment. Also, the charge population is mainly distributed on those C atoms adjacent to the V atoms, which leads to larger structural distortion in this region in C_{60}.

The isodensity surfaces of HOMOs and LUMOs of the lowest-energy structures of $V_n(C_{60})_m$ are plotted in Figure 7. It is evident that the HOMOs are mainly localized on the d (d_{xy}, $d_{x^2-y^2}$, d_{xz}, d_{yz}, d_{z^2}) orbitals of V atoms, whereas the LUMOs are mainly on the p_π orbitals of C_{60} in all of the sandwichlike complexes. However, different hybridization behavior is found for VC_{60} and $V_4(C_{60})_4$, where the d orbitals of V atoms are also found in the LUMOs.

More interestingly, the isodensity surfaces of HOMOs and LUMOs of the sandwichlike structures show strong similarities: the isodensity surface of "$V(C_{60})_2$" is also seen in both HOMOs and LUMOs of larger clusters of $V_2(C_{60})_3$ and $V_3(C_{60})_4$. The HOMO/LUMO isodensity surface of multidecker sandwichlike complexes can be constructed on the basis of that of $V(C_{60})_2$. For example, the isodensity surface of the HOMO of $V_3(C_{60})_4$ can be viewed as approximately two HOMOs of $V(C_{60})_2$ connecting by the HOMO of a V atom, and its LUMO is mainly from the middle two C_{60} molecules. On the basis of its BE per V atom, HOMO−LUMO gap, and VIP, $V(C_{60})_2$ is likely the most stable complex. The similarity of the HOMO/LUMO isodensity surfaces for the sandwichlike complexes suggests that $V(C_{60})_2$ can serve as a base for building larger sandwichlike complexes by adding additional VC_{60} units. Conversely, this view can also explain why $V_3(C_{60})_4$ has the smallest ion intensity in the mass spectra[3,30,31] because it tends to dissociate into a $V(C_{60})_2$ base plus two VC_{60} units or one $V(C_{60})_2$ base plus a smaller $V_2(C_{60})_3$ complex.

IV. Conclusions

We have studied structural, electronic, and magnetic properties of $V_n(C_{60})_m$ (n, $m \leq 4$). In general, the linear η^6-ligand sandwichlike structures are energetically more favorable than the η^5-ligand structures or nonlinear structures for (n, $n + 1$). However, for (1, 1), the most stable structure is a η^5-ligand conformation, and for (4, 4), a riceball-like structure is favored over a ringlike structure. The HOMO−LUMO gaps of these complexes are all relatively small, suggesting that they may be of high reactivity. The average binding energy per V atom and vertical ionization potential peak at (1, 2) and (4, 4). The lowest-energy structures are generally in their lowest spin state, except for (1, 1). Complexes in η^5-ligand configuration tend to be in high spin state.

Acknowledgment. This work is supported by the National Nature Science Foundation of China (nos. 10604013, 20873019), the Program for New Century Excellent Talents in the University of China (NCET-06-0470), the project sponsored by SRF for ROCS, SEM, the Qinglan Project in the University of Jiangsu Province, and the Outstanding Young Faculty and Peiyu Funding of Southeast University. We thank the computational resource at the Department of Physics, Southeast University. X.C.Z. acknowledges the support by the NSF (CHE, CMMI, and DMR/MRSEC) and the Nebraska Research Initiative.

Supporting Information Available: The energy difference of different spin states of the different structures of $V_n(C_{60})_m$. This material is available free of charge via the Internet at http://pubs.acs.org.

References and Notes

(1) Long, N. J. *Metallocenes: An Introduction to Sandwich Complexes*; Blackwell Science: Oxford, U.K., 1998 and references therein.

(2) Kurikawa, T.; Takeda, H.; Hirano, M.; Judai, K.; Arita, T.; Nagao, S.; Nakajima, A.; Kaya, K. *Organometallics* **1999**, *1*, 8–1430.

(3) Nakajima, A.; Kaya, K. *J. Phys. Chem. A* **2000**, *104*, 176.

(4) Miyajima, K.; Yabushita, S.; Knickelbein, M. B.; Nakajima, A. *J. Am. Chem. Soc.* **2007**, *129*, 8473.

(5) Zheng, W. J.; Nilles, J. M.; Thomas, O. C.; Bowen, K. H., Jr. *Chem. Phys. Lett.* **2005**, *401*, 266.

(6) Jaeger, T. D.; Heijinsbergen, D. V.; Klippenstein, S. J.; Helden, G.; Meijer, G.; Duncan, M. A. *J. Am. Chem. Soc.* **2004**, *126*, 10981.

(7) Rao, B. K.; Jena, P. *J. Chem. Phys.* **2002**, *117*, 5234.

(8) Gerhards, M.; Thomas, O. C.; Nilles, J. M.; Zheng, W. J.; Bowen, K. H., Jr. *J. Chem. Phys.* **2002**, *116*, 23.

(9) Knickelbein, M. B. *J. Chem. Phys.* **2006**, *125*, 044308.

(10) Rayane, D.; Allouche, A. R.; Antoine, R; Broyer, M.; Compagnon, I.; Dugourd, P. *Chem. Phys. Lett.* **2003**, *375*, 506.

(11) Meyer, F.; Khan, F. A.; Armentrout, P. B. *J. Am. Chem. Soc.* **1995**, *117*, 9740.

(12) Lyon, J. T.; Andrews, L. *J. Phys. Chem. A* **1997**, *109*, 431.

(13) Yasuike, T.; Yabushita, S. *J. Phys. Chem. A* **1999**, *103*, 4533.

(14) Froudakis, G. E.; Andriotis, A. N.; Menon, M. *Chem. Phys. Lett.* **2001**, *350*, 393.

(15) Pandey, R.; Rao, B. K.; Jena, P.; Blanco, M. A. *J. Am. Chem. Soc.* **2001**, *123*, 3799.

(16) Kandalam, A. K.; Rao, B. K.; Jena, P.; Pandey, R. *J. Chem. Phys.* **2004**, *120*, 10414.

(17) Wang, J.; Jellinek, J. *J. Phys. Chem. A* **2005**, *109*, 10180.

(18) Wang, J.; Acioli, P. H.; Jellinek, J. *J. Am. Chem. Soc.* **2005**, *127*, 2812.

(19) Maslyuk, V. V.; Bagrets, A.; Meded, V.; Arnold, A.; Evers, F.; Brandbyge, M.; Bredow, T.; Mertig, I. *Phys. Rev. Lett.* **2006**, *97*, 097201.

(20) Xiang, H. J.; Yang, J. L.; Hou, J. G.; Zhu, Q. S. *J. Am. Chem. Soc.* **2006**, *128*, 2310.

(21) Zhang, X.; Wang, J. *J. Phys. Chem. A* **2008**, *112*, 296.

(22) Kua, J.; Tomlin, K. M. *J. Phys. Chem. A* **2006**, *110*, 11988.

(23) Zhou, J.; Wang, W. N.; Fan, K. N. *Chem. Phys. Lett.* **2006**, *424*, 247.

(24) Xu, Z. F.; Xie, Y.; Feng, W. L.; Schaefer, H. F. *J. Phys. Chem. A* **2003**, *107*, 2716.

(25) Irigoras, A.; Mercero, J. M.; Silanes, I.; Ugalde, J. M. *J. Am. Chem. Soc.* **2001**, *123*, 5040.

(26) Swart, M. *Inorg. Chim. Acta* **2007**, *360*, 179.

(27) Schildcrout, S. M. *J. Am. Chem. Soc.* **1973**, *95*, 3846.

(28) Nagao, S.; Kato, A.; Nakajima, A.; Kaya, K. *J. Am. Chem. Soc.* **2000**, *122*, 4221.

(29) Zhou, L.; Yang, S.; Ng, M.; Sullivan, M. B.; Tan, V. B. C.; Shen, L. *J. Am. Chem. Soc.* **2008**, *130*, 4023.

(30) Nakajima, A.; Nagao, S.; Takeda, H.; Kurikawa, T.; Kaya, K. *J. Chem. Phys.* **1997**, *107*, 6491.

(31) Nagao, S.; Kurikawa, T.; Miyajima, K.; Nakajima, A.; Kaya, K. *J. Phys. Chem. A.* **1998**, *102*, 4495.

(32) Andriotis, A. N.; Menon, M.; Froudakis, G. E. *Phys. Rev. B* **1999**, *60*, 4521.

(33) Andriotis, A. N. *Phys. Rev. B* **2000**, *62*, 9867.

(34) Becke, A. D. *J. Chem. Phys.* **1988**, *88*, 2547.

(35) Lee, C.; Yang, W.; Parr, R. G. *Phys. Rev. B* **1988**, *37*, 785.

(36) DMOL is a density functional theory program distributed by Accelrys, Inc. Delley, B. *J. Chem. Phys.* **1990**, *92*, 508; **2000**, *113*, 7756.

(37) James, A. M.; Kowalczyk, P.; Langlois, E.; Campbell, M. D.; Ogawa, A.; Simard, B. *J. Chem. Phys.* **1994**, *101*, 4485.

(38) Langridge-Smith, P. R. R.; Morse, M. D.; Hansen, G. P.; Smalley, R. E *J. Chem. Phys.* **1984**, *80*, 593.

(39) Dresselhaus, M. S.; Dresselhaus, G.; Eklund, P. C. *Science of Fullerenes and Carbon Nanotubes*; Academic Press: San Diego, CA, 1996.

(40) Hedberg, K.; Hedberg, L.; Bethune, D. S.; Brown, C. A.; Dorn, H. C.; Johnson, R. D.; Veries, M. D. *Science* **1991**, *254*, 410.

(41) Wu, X. Y.; Ray, A. K. *J. Chem. Phys.* **1998**, *110*, 2437.

JP8064272